Journal of Theoretical Biology 409 (2016) 47–59

Contents lists available at ScienceDirect

Journal of Theoretical Biology

journal homepage: www.elsevier.com/locate/yjtbi

Chaos in collective health: Fractal dynamics of social learning

Christopher Keane *

Behavioral and Community Health Sciences, Graduate School of Public Health, University of Pittsburgh, USA

HIGHLIGHTS

- A model of collective health protection produces fractal patterns of disease.
- The model results in an exponential distribution of collectives of protectors.
- The time trace of infection is anti-persistent, reflecting negative feedback.
- The self-similarity coefficient corresponds to the level of health protection.

ARTICLE INFO

Article history:
Received 1 December 2015
Received in revised form
19 August 2016
Accepted 30 August 2016
Available online 31 August 2016

Keywords:
Health behavior
Collective behavior
Infectious disease
Chaos
Oscillations
Social learning

ABSTRACT

Physiology often exhibits non-linear, fractal patterns of adaptation. I show that such patterns of adaptation also characterize collective health behavior in a model of collective health protection in which individuals use highest payoff biased social learning to decide whether or not to protect against a spreading disease, but benefits of health are shared locally. This model results in collectives of protectors with an exponential distribution of sizes, smaller ones being much more likely. This distribution of protecting collectives, in turn, results in incidence patterns often seen in infectious disease which, although they seem to fluctuate randomly, actually have an underlying order, a fractal time trend pattern. The time trace of infection incidence shows a self-similarity coefficient consistent with a fractal distribution and anti-persistence, reflecting the negative feedback created by health protective behavior responding to disease, when the benefit of health is high enough to stimulate health protection. When the benefit of health is too low to support any health protection, the self-similarity coefficient shows high persistence, reflecting positive feedback resulting the unmitigated spread of disease. Thus the self-similarity coefficient closely corresponds to the level of protection, demonstrating that what might otherwise be regarded as "noise" in incidence actually reflects the fact that protecting collectives form when the spreading disease is present locally but drop protection when disease subsides locally, mitigating disease intermittently. These results hold not only in a deterministic version of the model in a regular lattice network, but also in small-world networks with stochasticity in infection and efficacy of protection. The resulting non-linear and chaotic patterns of behavior and disease cannot be explained by traditional epidemiological methods but a simple agent-based model is sufficient to produce these results.

1. Introduction

Health is a collectively shared benefit when an individual, by virtue of being healthy, confers benefit to local contacts who interact with that person. An individual's health allows them to engage in transactions for work or play, and therefore benefits others. But while each person's health is a social support to others, offering a collective benefit, each person's health often depends upon protective behavior that is in some ways costly, for example time and effort devoted to exercise, washing hands after interactions, or socially isolating oneself. That is, protection assures health as long as one protects, but incurs some immediate perceived cost, including time required to perform the behavior, e.g. time to wash hands, discomfort or embarrassment in wearing a facemask, or using a condom. "Defectors" pay no cost, because they are not taking protective action, but they will become infected if they have any infected neighbors. Thus a fundamental public health dilemma is that an individual can avoid the cost of health protection, yet can benefit from the health of others (free-ride) and therefore cooperative protection is vulnerable to collapse. This rests on the assumption that individuals do not automatically and rationally adopt health protective action due to possessing

* Correspondence to: 130 DeSoto Street, Pittsburgh, PA 15261, USA.
E-mail address: crkcity@gmail.com

http://dx.doi.org/10.1016/j.jtbi.2016.08.039
0022-5193/

knowledge of disease and its risks, but rather see protection as a behavior that has associated costs as well as benefits, and these costs and benefits include a variety of social as well as physical health factors (Funk et al., 2010). From this perspective, individuals learn not just by acquiring knowledge of disease, but rather by social learning (Festinger, 1954; Aberg Yngwe et al., 2003). One may learn though social learning, by observing behaviors of local neighbors. For example, one's local neighbors can serve as a behavioral example, supporting social learning of either health protection or defection (no health protection). While the public health literature emphasizes social learning and social networks (Berkman and Kawachi, 2000; Glanz et al., 2002; Berkman and Glass, 2000), the field has not produced models capable of showing dynamics such as local feedback in networks that are likely to result. In fact, such local learning can result in local clustering in behavior which in turn can produce local negative feedback effects, for example defection may spread, leading to the collapse of protection, but then the very success of the free-riding may extinguish itself locally. The success of protection in extinguishing local disease subsequently may lead individuals to defect. In turn, this increase in defection opens up vulnerability to disease. Thus there are multiple negative feedback mechanisms operating, protection responding to disease, defection responding to protection, and disease responding to lack of protection (defection). I claim the behavioral component of the feedback, driven by social learning, can over-react initially and that subsequent corrections produce oscillations at multiple scales. The errors resulting from the social learning strategy thus may be an important part of the explanation for the multiscale oscillations in patterns of incidence characteristic of chaos. For example, incidence of some childhood diseases have demonstrated multi-scale fractal irregularity over time (Holdsworth et al., 2012), as have rotavirus (Jose and Bishop., 2003), campylobacter (Skjerve and Glattre, 2006), measles (Bolker and Grenfell, 1996) and some cancers (Nygard and Glattre, 2003).

The social learning strategy I examine, adopting the locally highest payoff, also called highest payoff bias, "imitate the best," (Baldini, 2013) or copy-successful-individuals (Hoppitt and Laland, 2013; mesoudi, 2008), is common among humans and animals (mesoudi, 2008; Sarin and Dukas, 2009; Henrich and Broesch, 2011; Pasqualone and Davis, 2011; Seppanen et al., 2011; Mason, 1988; Kendal et al., 2009; Garcia-Retamero et al., 2009) and relatively adaptive to changing local conditions (Rendell et al., 2010) but, as are all social learning strategies in some way, it is also inherently biased (Boyd and Richerson, 1985; Hoppitt and Laland, 2013; Rendell et al., 2010; Baldini, 2013). In general, the biases inherent in the "adopt the highest payoff" social learning strategy can lead individuals to adopt suboptimal behaviors (Rendell et al., 2010; Schlag, 1998; Schlag, 1999; Denrell, 2005). This error is largely due to limitations in individuals' ability to predict payoffs associated with behaviors. Directly monitoring payoffs and behaviors of all individuals is often costly or difficult, and so individuals often must restrict observation to local neighbors. If it is not feasible to "directly" monitor payoffs, then an alternative strategy is to indirectly monitor some proxy for the payoff, such as health or wealth (Boyd and Richerson, 1985), but the main point here is that it likely is very costly or not possible to monitor much more than this local current sample. We will assume that asocial personal sampling of behaviors through trial and error (trying different behaviors and perhaps getting sick) is also costly, as often has been found true (Hoppitt and Laland, 2013; Valone, 2007; Morris, 1992). Observing only the highest local payoff, directly or indirectly, is a low cost and low difficulty strategy relative to monitoring a larger set of payoffs or monitoring all components of the payoff. However, this set of biases also lead to mistakes, some of which can be quickly corrected but others of which will take a longer period of time.

We will see how this type of biased social learning also leads to later error correction at multiple scales, especially when disease conditions spread spatially. For this reason, highest payoff social learning may lead to fractal and chaotic spatial or temporal oscillations of behavior reflected in disease patterns. If this is true, there may be an analogy between local social learning and adaptive physiology, which often exhibits non-linear, fractal patterns of adaptation. It is possible that social learning may likewise show non-linear, fractal patterns of response to change in conditions. Chaotic behavioral patterns can result even in simple repeated spatial prisoner's dilemma games, as evident in Nowak and May's seminal model (Nowak and May, 1992). If in the presence of a spreading virus collective learning by social comparison shows such chaotic patterns, this may explain the type of patterns often seen in infectious disease. Many diseases seem to fluctuate randomly but could have an underlying order, a fractal and chaotic time trend pattern that in turn may reflect underlying patterns of the social learning of health protective behavior. In other words, a simple social learning strategy, adopting the highest payoff in a spatially clustered network may be a sufficient explanation of chaotic patterns in disease incidence. It is possible that even a deterministic version of this model in a regular network, without stochasticity of variables, will produce chaotic patterns. To explore these possibilities, I present a dynamic model in which individuals learn socially and disease spreads.

1.1. Model

In this "Infection–Protection Game," as I call it, each individual earns one unit of benefit b from K_H healthy neighbors. Being healthy oneself earns two units of benefit, based on the assumption that individuals value their own health more than neighbor's health. So an individual benefits from health of their own self: $b2S_H$, where S_H is zero or 1 (healthy or not).

Individuals can prevent spread of infection by taking protective action. To "protect" means to put a barrier between self and contacts, such that if either has a virus, the protective action blocks the spread for one round of play. Protection, however, has a cost c for each of one's K neighbors. For example, in a simple grid lattice, with $K=8$, an individual pays cost 8c if an individual is the only local person protecting, that is if all eight neighbors are not protecting.

This model applies to behaviors that protect against spread of illness while that behavior is adopted, e.g. facemasks prevent spread of respiratory illness while used (by contrast the benefits of vaccination lasts well past the time of behavior). The model thus applies to non-pharmaceutical protective behaviors such as facemask use, handwashing, or condom use, all known to reduce transmission of infections (MacIntyre et al., 2009), and applies to illnesses for which there is not lasting immunity. Several transmissible diseases, often caused by bacteria, do not produce an immune response in the body, e.g., sexually transmitted such as gonorrhea, syphilis and chlamydia. For these bacterial diseases, after antibiotic treatment is completed, individuals return to an unprotected, susceptible state. Humans also are unlikely to develop full immunity to some viruses, such as rotavirus and rhinoviruses that cause acute respiratory infections and the common cold (Merler et al., 2008). There are more than 100 recognized serotypes of Rhinovirus, the primary cause of common cold, and so individuals are unlikely to develop full immunity (Merler et al., 2008). Individuals can contract rhinovirus up to five to eight times a year (Goldmann, 2001). Recurrent protective behavior is necessary to prevent recurrent illnesses that spread.

Likewise, the costs of protection associated with behaviors such as handwashing or facemask wearing are proportional the period of the behavior, and recur with repeat behaviors. Individuals

perceive costs of using facemasks to include discomfort, ill-fit, inconvenience (when wanting to eat, speak or show facial expression etc.), or embarrassment (MacIntyre et al., 2009; Merler et al., 2008; Goldmann, 2001; Ferng et al., 2011; Weiss et al., 2007; Syed et al., 2003). Perceived costs associated with handwashing include the time it takes, distance to water or skin irritation (Voss and Widmer, 1997; Kuzu et al., 2005; Dubbert et al., 1990; Pittet et al., 1999; Larson, 1985; Shin and Moey, 2014). Perceived costs associated with condoms include discomfort, violation of perceived ethnic and religious norms against condoms, perceived stigma of condom use, and anxiety discussing condoms due to lack of trusting relationship with a partner (Sarkar, 2008; Crosby et al., 2005; Lefkowitz et al., 2004; Schenker and Rabenou, 1993; Anonymous, 2006; King et al., 2005). These costs and benefits recur when the protective behavior recurs, and cease when the protective behavior ceases (true for handwashing, facemask wearing and condom use). In turn, higher number of contacts requires higher frequency of the behaviors and so higher costs. Thus the model does not apply to behaviors, such as vaccination, that have a lasting benefit, immunity, and do not incur higher costs with higher contacts.

Several theories of health behavior change, such as the health belief model and transtheoretical (stages of change) model, posit that the costs and benefits of health behaviors influence health behavior, and these theories have been successfully applied to handwashing, facemask wearing and condom use (Shin and Moey, 2014; Al-Tawfiq and Pittet, 2013; Noar et al., 2000; Arden and Armitage, 2008). Likewise, individuals in the agent-based public health model I present consider costs and benefits of behaviors, but individuals learn the sum of costs and benefits of behaviors by observing neighbors' current action and payoff. In my model, individuals only consider the current situation, the current round of play. Healthy defectors surrounded by only healthy individuals experience the benefit of health but do not consider the risk of infection, because they see no neighbors currently infected. This roughly corresponds to the "pre-contemplation" stage of the stages of change model (Al-Tawfiq and Pittet, 2013; Noar et al., 2000; Naar-King et al., 2008) (Arden and Armitage, 2008; Prochaska and Velicer, 1997; Prochaska, 2008), in which individuals do not consider the costs of the unhealthy behavior. But defectors are likely to become infected, at which point they experience the cost of defection (loss of health), roughly corresponding to the "contemplation" stage. Infected defectors next to one or more health protectors may see that protection at this point earns a higher payoff than defection. This corresponds to the "determination" (or preparation) stage in which an individual determines a behavior to adopt that leads to a better outcome. Individuals who then adopt protection are in the "action" stage. Several health behavior theories emphasize the role of norms in adopting and maintaining a health action (Ajzen and Fishbein, 1980; Ajzen, 1991). Corresponding to this, if a health protector is surrounded by other health protectors, they gain positive social support and social approval for complying with a norm (earning a benefit roughly proportional to the number of healthy neighbors). So long as a protector does not see defectors with higher payoffs, the protector is not tempted to defect, and protection is maintained, corresponding to the "maintenance" phase. But a protector defects if they are next to a defector earning the highest payoff, corresponding to "relapse". These examples show how individuals might move through stages of decision making based on costs and benefits learned from neighbors in a network.

The model accounts for social norm compliance, by including a 50% cost reduction for protection when a neighbor is protecting, e.g., an individual who has decided to protect and who has only one neighbor who is protecting ($K_P=1$) pays a cost $c(K-K_P/2)=$ 8c–1c/2=7.5c. If all eight of one's neighbors are protecting ($K_P=8$) then an individual only pays $c(K-K_P/2)=8c-8c/2 = 4c$ for protecting. This is based on the assumption that protective actions are less costly when one's neighbors are also taking protective action. In other words one pays 50% more cost for non-compliance with a local norm of protecting. I generalize this as a cost saving of $K_P/2$ for each pair of protectors. In sum, the total payoff per person is:

$$b(2S_H + K_H) - c(K - K_P / 2)$$

Infection spreads between unprotected neighbors. If infected individuals do not protect, then the infection spreads to their unprotected neighbors with a probability equal to the infectivity. Infected individuals retain the infection and are infectious for a duration d of iterations, then after one time step of immunity they return to a state that is susceptible to re-infection (the disease confers no long-term immunity, which we simplify as an immunity period of 1 iteration). This produces a susceptible-infectious-recovered-susceptible (SIRS) dynamic that characterizes many sexually transmitted diseases, e.g. gonorrhea, for the majority of communicable diseases transmitted by Helminth or bacterial agents, and the common cold (Brauer and Castillo-Chavez, 2012). However, the infect-protect model emphasizes behavioral dynamics in disease spread, specifically a behavioral protection decision that may mitigate spread of the disease. At each round of play, individuals choose whether or not to protect, to block the spread of infection between self and neighbors, but that action has a one unit cost for each neighbor. This is an abstraction of the idea that in non-pharmaceutical measures such as handwashing and facemask wearing, the behaviors are roughly proportional to the number of one's contacts. Once one is away from all contacts, one need not wear a facemask or wash hands. If an individual encounters contacts only during a brief visit to a grocery store, one puts on a mask during that time, and washes hands afterwards. However, if one comes in contact with many others throughout most of the day, one must wash hands or wear a mask throughout the day. Somewhat similarly, one who has multiple sexual contacts must more repeatedly use a condom.

At every round of play, individuals observe the total payoff for all local individuals, including themselves and their eight surrounding neighbors. Individuals, only seeing their local immediate condition, recalculate their short-term payoffs at each step as the sum of current benefits minus costs. Each individual imitates the neighbor with the highest payoff. Thus the game is an evolutionary spatial game, as in the spatial prisoner's dilemma model (Nowak and May, 1992). Each step of the game, individuals adopt the action taken by the local individual with the highest current payoff. This is analogous to an evolutionary process in which individuals with the highest payoff are more likely to survive. For example, if a protecting individual has a higher payoff than any of their eight neighbors they survive, as a protector, into the next round of play. The individuals in this model do not rationally calculate all possible payoffs, but rather are only aware of local results. Each individual can only know the most recent actions and payoffs of their own and of their immediate neighbors. Can such myopic individuals learn to protect themselves and others from infection?

2. Methods

2.1. Game in networks

I programmed the game and iterated it in a variety of population structures, which I modeled as graphs (Kearns, 2007; Lieberman et al., 2005; Jackson, 2008; Wilensky, 1999). Individuals occupy the vertices of an undirected graph, a square lattice, and

interact directly only with their neighbors, connected via "edges," in a neighborhood. I simulated the infect-protect game on a regular graph (grid lattice), and also small-world networks, which are regular graphs with sufficient proportion of edges rewired to produce small-world properties. The regular grid lattice network I used was a 101 by 101 two-dimensional lattice of individual agents (10,201 individuals), each with eight local neighbors (a Moore neighborhood). Each patch in the grid is occupied a single individual which, at the start of the game, is protecting or defecting at random. More specifically, before the game begins, the distribution of protectors is 50% in the grid lattice, and the remaining 50% of individuals are defectors. A random 10% of individuals are infected. The behaviors and infection are randomly distributed spatially. I examined the average level of protection over 500 time steps for every level of infectivity from 0% to 100% at 1% increments. We want to examine a range of infectivity, in part because infectivity varies greatly by specific disease and mode of transmission [62.63]. I also determined the level of protection for every level of benefit to cost ratio. For the latter I held the cost constant at $c=1$, and varied b, starting with $b=1$, and increasing by 0.1 up to a level of $b=6$. For each level of b, I iterated the game 500 times, recorded and plotted the proportions and distribution of protection, infection and defection. When examining the effects of how the b/c ratio varies by network structure I ran analysis for each of two levels of infectivity, one case where disease spreads with 100% infectivity and another case where infectivity is only 6%, in the absence of protection. For analysis of sizes of collectives and for wavelet analysis, where more data points are helpful, I iterated the game 6000 steps for each condition tested.

2.2. Game beginning with a block of protectors

To elucidate under what conditions, e.g. level of benefit and cost, collectives of protectors are viable, I also ran the model starting with a block of protectors. We start with a 5×5 block of protectors, all healthy, at the center of the grid, otherwise occupied by infected defectors. Then, running the model for a complete range of benefit to cost ratios, e.g. setting $c=1$, and incrementing b by 0.01 for each run of 6000 iterations, we can determine what level of b/c is supportive of protection. Infectivity is 100%. This version of the model is deterministic, like a cellular automata, because there is no random distribution of any of the variables nor stochasticity in actions, and thus also can demonstrate whether deterministic chaos results. If so, then chaotic oscillations in incidence of infection need not depend on randomness of variables. Chaotic oscillations may result from a deterministic game with feedback.

The infection–protection model results in many local collectives of protection that are surrounded by defectors (visible as blue islands of protection in Fig. 1), motivating the quantification of the numbers of these collectives and their sizes. I modified an existing algorithm (Sarin and Dukas, 2009; Henrich and Broesch, 2011; Pasqualone and Davis, 2011) to identify collectives of protection on the 2-dimensional lattice (Hjorth et al., 2014; Kanungo et al., 2002; Coates and Ng, 2012). However, to avoid confusion with the term clustering as used in network analysis, I use the term "collectives". Protective collectives in this paper are defined as collections of one or more individuals who are protecting (not defecting) and, crucially, if a protecting individual is next to one or more other protecting individuals they must belong to the same collective. The algorithm finds the number of collectives by partitioning the observations into n collectives, in our case collectives of protection, where n refers to the number of collectives the algorithm looks for initially. The algorithm works by finding the average position of the protectors in n different collectives. It starts by simply guessing an average position for each of the n collectives, and then improves these guesses as it iterates the algorithm. The result of that algorithm is a set of n points (n "centroids"), each of which is located at the average position of a corresponding collective. Each collective is assigned an arbitrary but unique number, thus counting the number of individuals belonging to each collective is straightforward. At each time step of the infection–protection game, the algorithm identifies separate collectives, and then the sizes of the collectives are computed and recorded. The modified algorithm keeps a running cumulative list of the sizes of collective, updated at each game play, and then computes the total cumulative number of collectives of each possible size: 1, 2, 3 … 10,201 (max possible size comprising the entire 101×101 lattice).

2.3. Adding small-world network properties

Many social networks are structured as small-world networks, in which the average path length between pairs of individuals is relatively low, and yet the clustering remains relatively high, close to the level in a grid lattice (Watts and Strogatz, 1998; Telesford et al., 2011). For any individual in the grid that has no rewirings, the proportion of one's neighbors that know each other is 42.9%. This degree of clustering of the networks we examine approximates that found in many real social networks (Watts and Strogatz, 1998; Telesford et al., 2011) and has often been found to be the underlying network structure in which various health behaviors spread (Centola, 2010; Christakis and Fowler, 2009). Randomly rewiring some local connections in a grid lattice lowers the clustering coefficient only slightly but also lowers the average path length. With enough rewiring the lattice acquires small-world properties (Watts and Strogatz, 1998). Whereas the straight lattice has a high clustering coefficient and an average shortest long path-length between pairs of individuals (and so is a large world), the rewiring lowers not only the clustering coefficient but also the path length, so for example this lowers the number of steps it would take for an infection to spread throughout the network. Health behaviors spread differently in a random versus a grid-lattice network. For example, an experiment manipulating network structure found that health behavior spread further and faster through clustered-lattice networks compared to random networks (Centola, 2010). Thus, our comparison of a random vs. a grid-lattice network is likely to show different dynamics in the spread of behavior. Moreover, it is possible that the infect-protect game model may produce chaotic oscillations in health protection and disease incidence in clustered lattice networks but not in small-world networks. Therefore, we compare results for these different network types.

To transform the lattice into a small-world network, I used the algorithm developed by Watts and Strogatz (1998) which randomly rewires a number x of the connections in a square grid lattice, while preserving the same average number of neighbors as in the lattice (which had a degree of $K=8$ in our case). The rewired lattice has the same total number of links and the same number of individuals as in the original regular lattice. The rewiring process randomly selects a link in the square lattice, and replaces it with a randomly selected link. The algorithm iteratively reconnects links until x number of connections are rewired. The outcome of this process is to slightly lower the clustering coefficient, the degree to which neighbors know each other, and to lower the path length. The random rewiring adds stochasticity to the initial conditions, since it will be slightly different every time. Therefore, I ran 25 simulations (6000 iterations for each of the 25 simulation runs) to account for variability in results. I varied the number of reconnections from $x=0$, $x=100$, $x=500$, $x=2000$, and $x=4080$ (10% of all connections). After rewiring the degree always remained at $K=8$. The rewired lattices had an average standard deviation of 0.992.

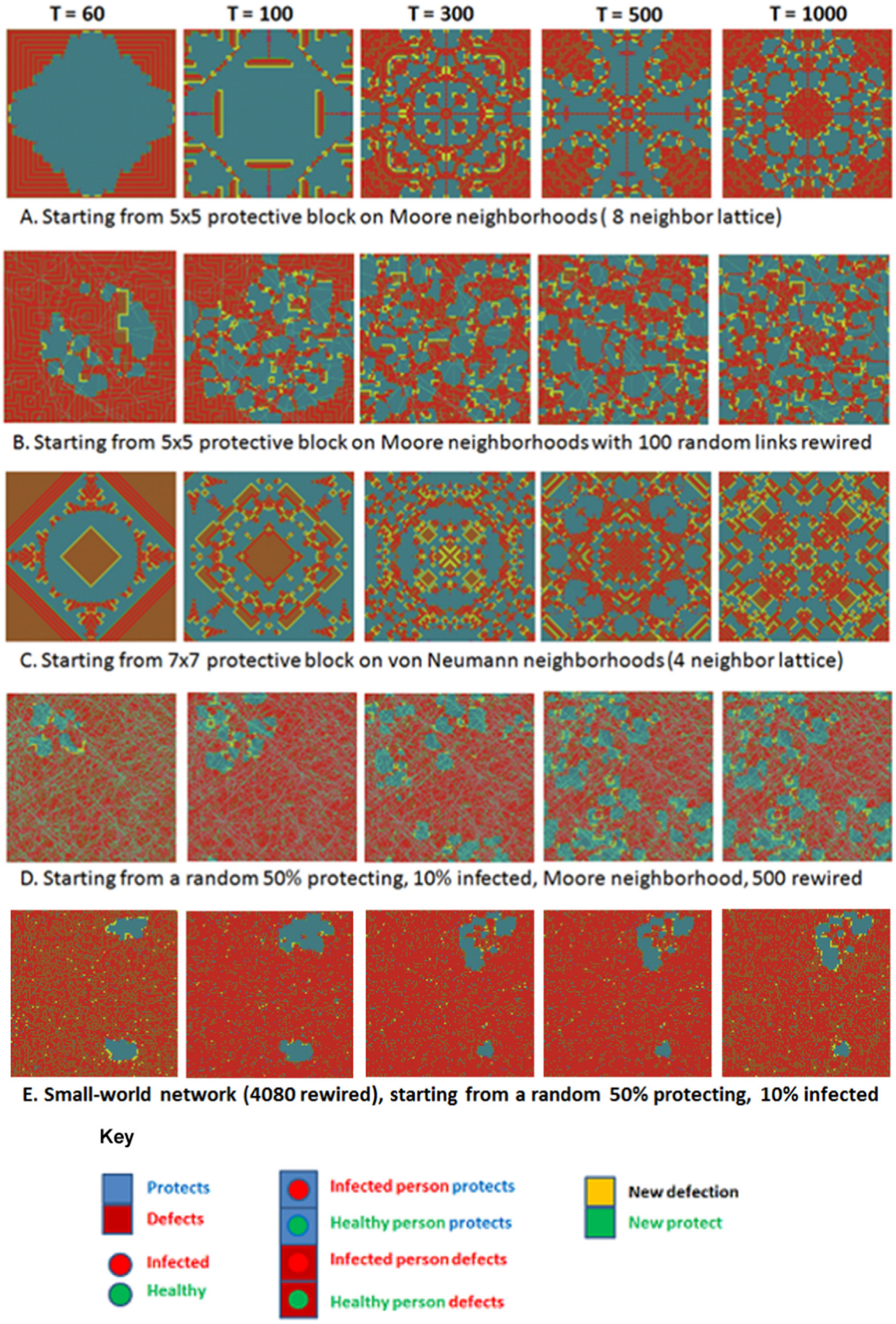

Fig. 1. Protection (blue) & defection (red) co-existing as virus spreads. (a) Results starting with a 5×5 block in a lattice network with $K=8$. Protection survives in small collectives when the b/c ratio is between 2 and 2.166. (b) Results on the $K=8$ lattice with 100 connections rewired. (c). Results in a $K=4$ lattice, starting with a 7×7 block (a 5×5 block of protection does not survive in a $K=4$ lattice). (d) a $K=8$ lattice, with 500 rewired connections, starting with a random 50% of individuals protecting and a random 10% infected. (e) Results in a small-world network (10% of connections rewired).

Using the small-world measure ω (Telesford et al., 2011), I quantify the degree of conformity to small-world properties, based on the clustering coefficient and path-length. This small-world measure compares the clustering coefficient of the rewired network to that in an equivalent lattice network (the original unrewired lattice network) and compares the path length of the rewired network to that in an equivalent random network (a random network with the same number of individuals and degree distribution as in our lattice network).. The equivalent random network is created by starting with the same number of individuals as in our lattice but no edges, then assigning an edge to node pairs with uniform probability and maintaining the degree distribution of the lattice network with 10% of links rewired (our candidate small-world network). The standard deviation of the degree was 0.992 in the equivalent random network and the average degree is $K=8$. Then the small-world measure, as defined by Telesford et al. (2011) is quantified specifically as

1. ω=LRand/L–C/CLatt
2. LRand is the path length of the equivalent random network.
3. L is the path length of the candidate small-world network (our rewired lattice network).
4. C is the clustering coefficient of the candidate small-world network.
5. CLatt is the clustering coefficient of the original lattice, with no rewiring, and a degree of $K=8$ (each individual has 8 neighbors).

A value of ω close to zero indicates strongly small-world properties, a value close to -1 indicates a network very close to a lattice, whereas a value close to $+1$ indicates a random network. In the 101 by 101 lattice with a random 10% of connections rewired randomly, the average path length is $L=6.41$, and the clustering coefficient $C=0.318$. In the straight lattice with no rewiring the clustering is $C_{Latt}=0.429$. In the equivalent random network, the average path length is 4.71. This yields a small-world index value of $\omega=-0.0065$, indicating strongly small-world properties.

2.4. Wavelet analysis to determine the self-similarity scaling exponent α

Self-similarity in oscillations is one characteristic of deterministic chaos. What seems to be random noise in incidence may actually have a type of order that is characteristic of chaos, namely a self-similarity across scales. This self-similarity, called fractional Brownian noise, is a frequency distribution of amplitudes of dips and peaks that has similarity across scales. If this self-similarity exists in the noise, it becomes evident once we scale up the sizes of changes in infection (amplitude) relative to time by a self-similarity scaling exponent (Addison, 1997). Roughly speaking the self-similarity scaling exponent α (Hurst exponent) indicates the degree to which one would need to scale up the change in infection relative to the scaling up of the time dimension. This exponent α indicates the scaling of the amplitude relative to the scaling of time that is necessary to preserve fractal self-similarity across scales, e.g. if time is scaled up by a factor S, then the amplitude is scaled up by a factor S^{α}. To calculate the self-similarity (Hurst) exponent, I submitted the infection time trace points to wavelet analysis. The game model simulations run for 6000 time steps and records the level of infection for each step. I submitted those time points to wavelet analysis using Benoit software (version 1.31). At each time step we have an average of changes in infection status, across all individuals in the grid. While the changes of each agent is based on a discrete model, the changes in the group averages from one step to the next, are a continuous Gaussian (bell-shaped) distribution. Taken alone this would seem only to reflect random changes, however there may be long-term persistence of trends that we may measure with the self-similarity coefficient, the Hurst exponent. The Benoit software calculates the Hurst exponent based on the input of discrete time-series data (which is "discrete-time fractional noise"). The wavelet algorithm used by Benoit uses Fourier analysis and estimates the self-similarity scaling parameter α. The wavelet analysis uses a random selection of 4096 time points because this number of data points analyzed must equal a power of 2. The analysis breaks the trace into 3 wavelet transforms, computing a separate variance for each and averaging these. The wavelet algorithm used by Benoit to estimate the self-similarity scaling parameter α and the fractal dimension D uses the first three wavelet transforms.

3. Results and discussion

3.1. General results

When $b>=2.0$ (and $c=1$), then protection survives alongside defection and infection, with all three oscillating (Figs. 1 and 2). That protection survives alongside defection and infection is shown in Fig. 2 over the course of 1–6000 iterations. Fig. 2 shows protection oscillating between about 25% and 70% starting after about 10 iterations and lasting through 6000 iterations. Protection survives in clusters of exponentially varying sizes (Fig. 3). Among the six conditions depicted in Fig. 4, there was only one that clearly did not support co-existence: the lattice when there is only 6% infectivity and duration of $d=5$ quickly brought infection down

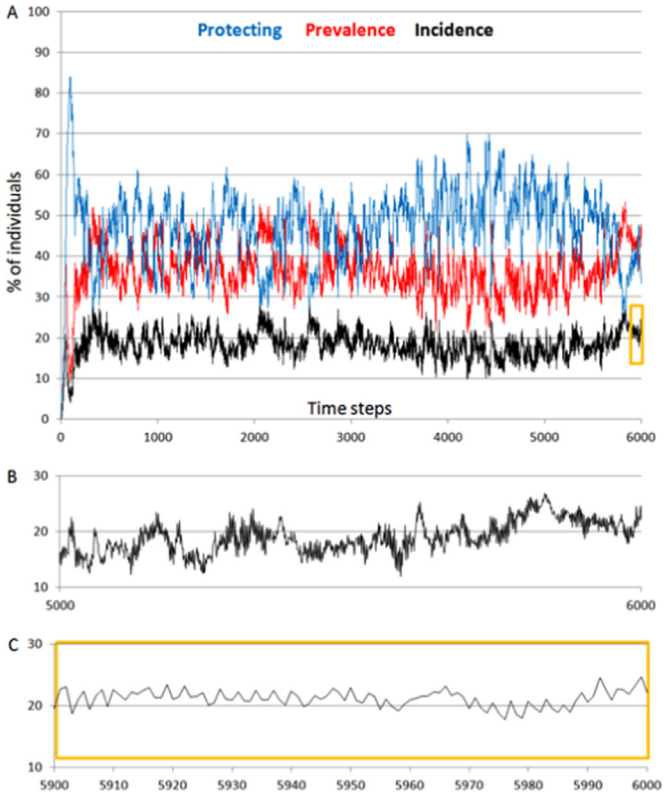

Fig. 2. Deterministic chaos in the infection–protection game. (A) Time trace of protective action (blue), prevalence (red) and incidence (black) of infection, corresponding to patterns depicted in Fig. 1a (local lattice, no rewiring). Levels of protective action over time oscillate chaotically. We obtain exactly these results for any b/c ratio between 2 and 2.166. (B) Closeup of incidence, (C) Closeup of yellow box in A, scaled-up according to the self-similarity scaling exponent $\alpha=0.104$ for incidence, where time is scaled up by a factor S of 60 times, the y axis showing amplitude scaled up by a factor $S^{\alpha}=1.5$.

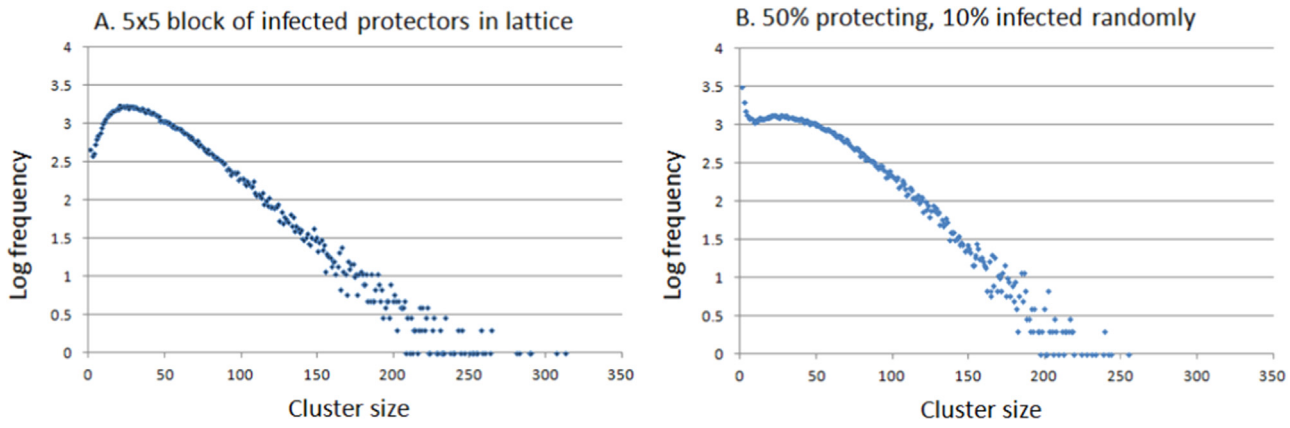

Fig. 3. When protection survives in collectives, smaller collectives are exponentially more likely. (a) Results when the run starts with a 5×5 block of protectors (as in Fig. 1a). Smaller collectives are exponentially more frequent, showing a relatively linear slope on a log-linear plot. (b) Results when starting with 50% individuals protecting and 10% infected, with protection and infection independently randomly distributed on the lattice. These results are the distributions over 6000 iterations.

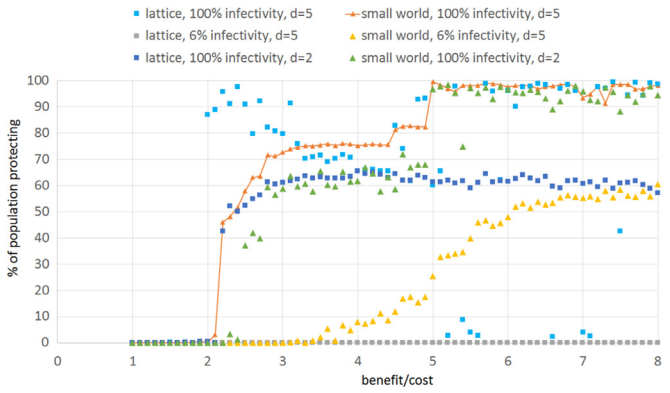

Fig. 4. Proportion protecting by size of the benefit/cost ratio, comparing results by network structure, infectivity and duration. Above a b/c of 2.166, protection can survive, but often protection and defection coexist, but increasing the size of b increases protection. Increasing of benefit, up to about $b=3$, increases the mean proportion protecting. Below a benefit of 2, protection never survives. These statistics summarize data over 500 game iterations for each b/c ratio.

to zero, after which protection went down to zero. Averaging together the results for the remaining five conditions (3 small-world networks and 2 lattice network conditions) shown in Fig. 4, at the final iteration ($t=500$), the mean percentage protecting was 84.5% (and so defection was 15.5%) and the mean percentage infected was 18.8%, showing co-existence through the 500 iterations. Starting the game with a randomly distributed 50% protecting, 50% defecting and 10% infected in the grid lattice, results in some blocks of protectors. That is, random chance produces some square blocks of protectors of size 3×3, size 5×5 etc. These blocks of protection can survive when the b/c ratio is at least 2, specifically when. $b >= 2.0$, holding c constant at 1. The protective blocks expand when b/c is greater than 2.166. This is true for both square lattices and also small-world network structures (as we will explore in more detail later), and is true for all levels of infection duration d. In all these cases, when the b/c ratio is equal or above 2, blocks of protection tend to grow in size wherever there is also local infection, whereas lone protectors tend to die out. Infection spreads where defection predominates, leading to a rise in protection. This pattern leads to oscillations, with protection rising in response to a prior peak in infection. The rise in protection brings down infection which leads to increased defection. This pattern repeats. Now let us quantify these qualitative results, starting with a results of an experiment isolating the role of a block of protectors, then submitting the oscillations to wavelet analysis.

3.2. Blocks of protection

What types of initial spatial clustering of behaviors can support co-existence of protection and defection? Protection can invade a population of defectors when we start with spatial blocks of 5×5 protectors who are infected (methods 2.2). Smaller blocks of protection cannot expand. When we start with a 5×5 block of infected protectors, then below a benefit to cost ratio of 2.0 ($b < 2.0$, $c=1$) protection expands briefly but protection does not survive beyond 96 iterations of the game, at which point infection takes over the population. If b is below 1.666, protection cannot expand at all. When we start with only a 5×5 block of healthy protectors within a square lattice, then above a b/c ratio of 2.166, protection takes over the entire population, eliminating disease. Between a ratio of 2 and 2.166 protection co-exists with defection and infection indefinitely (Figs. 1–3), forming transient collectives of protection, showing a fractal pattern over time, consistent with deterministic chaos, as we will examine below. These dynamic patterns do not repeat over time but manifest in exactly the same way for every simulation because the model is deterministic.

3.3. Conditions for takeover of population by protection or defection

Chaotic oscillations in behavior cannot occur under conditions supporting complete takeover of one behavior. Under what conditions should we expect protection or defection to take over the population? In pursuing this question, one approach is to determine the evolutionarily stable strategy (ESS), adapting the traditional concept of ESS to populations of finite size (Kearns, 2007; Ohtsukia and Nowak, 2008; Lieberman et al., 2005; Ohtsuki et al., 2006; Kearns and Suri, 2006). As an alternative approach, focusing on evolutionary dynamics, I will show levels of protection and defection that survive for various levels of b/c, and estimate extinction thresholds (Nowak and May, 1992; Nowak, 2004). Because protection and defection in my model also depend upon infection, I also compare the levels of protection and defection surviving for varied levels of duration of infection (d) and levels of infectivity.

We can predict the conditions for takeover of defectors starting with a single defector as did Nowak and May (1992) for a spatial prisoner's dilemma (Nowak and May, 1992). However, in our model we also have the interesting challenge of determining the conditions supporting takeover by defectors with and without presence of infection. Invasion of a population of protectors by a single healthy defector should be easier than infection by a single

infected defector. We can calculate exactly the b/c ratio that would prevent invasion by an infected defector, and compare that to the b/c ratio that would prevent invasion by a healthy defector.

Based on the payoff structure (Section 1.1) we expect protection to eliminate the single defector when $b/c > 4.5$. The defector pays no cost but is next to 8 healthy neighbors and so gains $8b$. The 8 neighboring healthy protectors each earn $9b$ (based on the formula described in Section 1.1), but each pays a cost for each neighbor. That cost is equal to 8 (a cost of 1 for each neighbor) minus the 50% discount for each protecting neighbor = 7/2 (each protector is next to 7 other protecting neighbors). Protectors bordering the defector earn $9b–4.5c$. Thus, the single defector will see that the neighboring protectors do better than defection if $9b–4.5c > 8b$. So if $b/c > 4.5$, the defector will protect instead of defect. If $b/c < =4.5$, the defector breaks even or does as well as neighboring protectors and so remains a defector. If $b/c < =4.5$, the defector survives, when there is no recovery from infection (that is if there's an unlimited duration of infection), but when b/c is greater than 2.0, the infected defector does not expand. This happens when a protector bordering a single infected defector, sees that the defector earns only $8b$, but will also see a neighboring protector earning $10b–4c$ which is a higher payoff than $8b$ when $b/c > 2.0$. When b is less than 2.0, an infected defector (temporarily) expands to a 3×3 block of defectors when infection has a long duration. The above results hold for infected defectors, strictly where there is no recovery from infection (or very long duration of infection). However, if the single infected defector recovers from infection then the healthy defection will expand and take over. If duration $d=2$ and $b/c < =4.5$ then once the single infected defector recovers, healthy defectors will grow. That is, a single infected defector, when b/c is less than 4.5 and duration is limited, will persist as a defector and also can recover from infection. Then defection will spread from the single healthy defector to the entire population of protectors.

A single defector is only one possible starting condition. Starting with a random mix of protectors and defectors we will by chance have some blocks of protectors of size 5×5. The critical situation is at the corners of the block. Defectors at the corner of the protective block switch to protection if $b/c > 2.166$, in the simulations (see results in Section 2.2, Fig. 4, and upper panel of Fig. 5). This is because defectors at the corners of the block of protectors (Fig. 6) see a maximum score for defection by a defector next to two protectors, and see a maximum score of protectors by a protector next to 3 other protectors. Thus the defector at the corner of the protective block will decide to protect if $5b–6.5c > 2b$, so $b/c > 6.5/3 = 2.166$ (Fig. 6). So a block of protectors within a sea of infected defectors will expand and take over if $b/c > 2.166$.

3.4. Sizes of local protective collectives

Local collectives of protection form, generally surrounded by defectors (Fig. 1). A collective of protection is defined as a group of one or more protectors who are linked directly to each other or linked via one or more other protectors. Protectors linked to each other in this way belong to the same protective collective. Collectives of protectors not linked to each other are separate, different collectives, In this way, we quantify the sizes of each protective collective arising over the course of 6000 iterations. Plotting the frequency of collectives of each size reveals an exponential frequency distribution (Fig. 3), except for collectives smaller than a 5×5 block of protectors, the smallest size sustainable over time. This exponential frequency distribution is consistent with deterministic chaos in nonlinear systems (Addison, 1997).

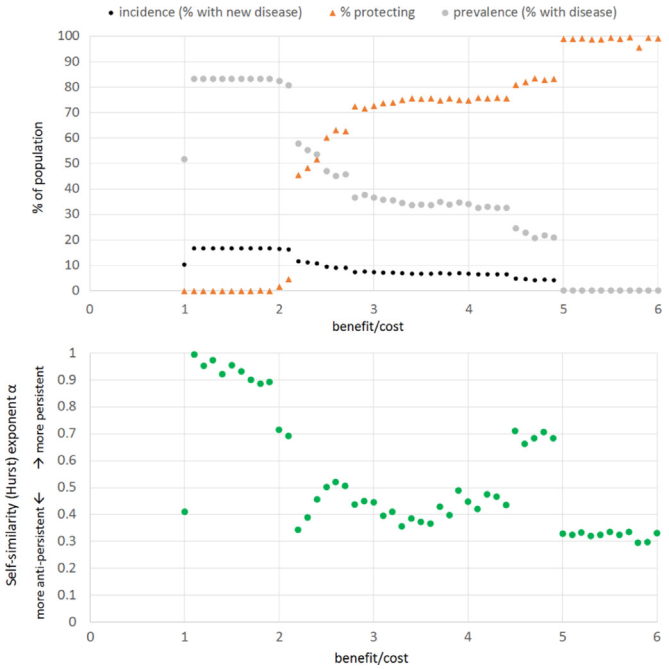

Fig. 5. Self-similarity exponent α reflects levels of protection. All data points represent averages over 6000 iterations. The network is small-world, duration of disease is $d=5$, infectivity = 100%. Upper panel: Where $b/c < 2$, protection does not survive (upper panel) and so α (lower panel) reflects only disease persistence. Where $b/c > 5$, the dynamic is largely protection reacting against any disease (anti-persistence, negative feedback). Where b/c is between 2 and 5, changes in levels of α correspond to changes in the proportion protecting, and negatively correspond to changes in disease. Average incidence varies little, but incidence fluctuations measured by α contains much information about protective responses to disease.

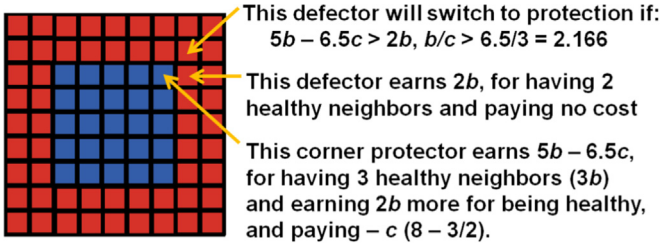

Fig. 6. Illustration of a condition leading to expansion of block of protectors. The defector bordering the protective at the top corner will switch to protection if any neighboring protector (which is only the top corner protector) earns more than any neighboring defector (which is the defector bordering two healthy protectors), which occurs if $b/c > 2.166$. Examining the other defectors bordering the block shows that at $b/c > 2.166$, the neighbor with the highest payoff always is a protector.

3.5. Effects of adding small-world network properties and lowering infectivity

Population structure, such as degree of network clustering, often affects behavioral dynamics (Pascual et al., 2011; Salathé and Jones, 2010). It is possible that degree of clustering will affect the game model's chaotic behavior. Clustering, the degree to which one's neighbors are in contact with one's other neighbors, is generally likely to affect behavioral dynamics. Important to the spread of behavior may be one's "core discussion group," a small number of persons with which one can discuss important or intimate matters (Marsden, 1987; Zhou, 2005). These "core discussion groups," also called "support cliques" generally have high clustering. Where there is clustering, interactions are not random (as in a random network) nor is there complete mixing, but rather an individual's neighbors know many of one's other neighbors, and individual's tend to share the same social situation and

disease conditions with one's neighbors. In the infect-protect game, clustering of protectors lowers the interface with exploiting defectors. Since individuals can only learn locally, if they are inside a protective cluster they see only other protectors, and they see no defection to tempt them. However, at the boundaries of the clusters, protectors see defectors and their payoffs. The $K=8$ grid lattice (Moore neighborhood) has a clustering coefficient of 0.429, meaning that one's neighbors on average know 42.9% of one's other neighbors.

Running the game on a Moore neighborhood that has been subjected to 100 rewirings reducing the clustering coefficient to approximately 0.426, protection survived for indefinitely long periods in all of 25 simulations (Fig. 1b shows an example), but does not eliminate infection completely. Rewiring 500 connections, the clustering coefficient is approximately 0.414, and protection survived indefinitely (Fig. 1d shows an example) in 88% of the simulations (22 of 25 simulations). Rewiring 2000 connections (about 5% of all connections) and protection survives indefinitely 64% of the time (16 of 25 simulations). If we rewire 10% of connections, we obtain small-world properties, as explained above in Methods. We explore results in a small network in detail below. This is important because if health protection is not viable in small-world networks then the chaotic behavioral oscillations we see in the square lattice networks will collapse in small-world networks. Remarkably, the small-world network structure is more supportive of protection than square lattice, over a wide range of conditions. When infectivity is only 6%, levels of protection are higher in the small-world networks than in the lattice at all levels of b/c (Fig. 4). For certain b/c ratios the small-world network is more supportive of protection than is the lattice at all levels of infectivity (Fig. S1). The (unrewired) lattice network tends over time to produce clusters of protection, defection and so also results in clusters of infection. Over time infection tends to exist in clusters in a lattice, specifically clusters of defectors. Rewiring tends to disperse infection. Moreover, distance (average path length) is higher in the straight lattice network (hence a "large" world) compared to the small-world network (Watts and Strogatz, 1998; Telesford et al., 2011). In the grid lattice, compared to a rewired network, infection takes more steps to travel throughout the network because the average path length is greater. Randomly rewiring the lattice lowers the average path length and individuals on average in the small-world network have less distance from infection. Because infection spreads to only to defectors, the rewiring disrupts clusters of healthy defectors by increasing infection. Thus the small-world networks (lattices with 10% rewiring) lowers the benefit of defection by undermining the clusters of healthy defectors that have an easier time surviving in straight lattices. For these reasons defection does not do as well in the small-world network. Defection is vulnerable to infection, and so we see higher levels of protection surviving in the small-world network.

Lower infectivity also helps defection and so lowers the proportions of protection surviving, because defectors are more likely to be healthy and so to earn a higher payoff. For this reason, defection earns a higher immediate payoff when infectivity is lower, and so protection is less likely to survive. In sum, two factors that help defection, and thus lower the viability of protection, are greater distance from clusters of infection and lower infectivity. To inspect this effect more closely, I also compared results for the lattice and the small-world structure for different levels of duration and infectivity. Running simulations of the infect-protect game in a small-world network with much lower infectivity (6%) and longer duration of infection (5 time steps), as well as a $b/c=5$, yields a somewhat more realistic situation than a square lattice and 100% infectivity. When infectivity is only 6%, duration of infection=5, protection did not survive in square lattice networks with no rewiring. Defection and infection took over the population, to the detriment of the collective welfare. Running the simulation 25 times, protection never survived (past 17 steps). By contrast, in a small-world networks (a lattice with 10% of edges rewired), when b/c is above 3, then further increases of b/c ratios resulted in higher proportion of protection surviving (Fig. 4), which led to lower overall levels of infection in the small-world compared to the lattice network. Perhaps the most striking result is that for low infection (6%) protection is viable in small-world networks but not viable in the straight lattice network.

3.6. Time trace patterns

Analyzing the oscillations of protection and incidence of infection shows that they vary chaotically, meaning the oscillations are aperiodic, even when the model is deterministic (Fig. 2). This apparent random noisiness of the chaotic oscillations nonetheless have a type of fractal order, self-similarity across scales, fractional Brownian noise, as described under methods. For a time trace of pure fractional Brownian noise $\alpha=0.5$ and the corresponding fractal dimension $D=2-\alpha$, or 1.5). Values of $\alpha<0.5$ indicate much folding such that we can see, at the larger scale, the time trace frequently turns back upon itself rather than persisting up or down, and within each larger scale fold we see similar folding at smaller scales, which tends to keep the divergent oscillations within bounds. α also indicates the degree to which the time trends are persistent or anti-persistent. For example, the time trace for infection might be anti-persistent, if a rise in infection triggers some immediate protective action that brings infection back down resulting in anti-persistence due to negative feedback, at least when infection has a brief duration. Anti-persistent time trend data will have $\alpha<0.5$, which we can intuitively understand as more jagged (rough and folded) time traces at all scales, whereas persistent data will have $\alpha>0.5$ (smoother trends). The fractal dimension of the time trend D_W is simply 2 – α.

When the game starts with 5×5 protecting block (as in Fig. 1a) using the 6000 time trace data points shown in Fig. 3, protection has $\alpha=0.643$, and a corresponding fractal dimension $D_W=1.357$. Thus the time trace for protection is more persistent than regular Brownian noise. Incidence shows a level of α that is quite anti-persistent, with $\alpha=0.105$.

When starting conditions are a random 50% of individuals protecting, and a random 10% of individuals infected (as in Fig. 1d), the mean self-similarity coefficient for infection, $\alpha=0.292$ (SD=0.247). Overall the pattern is quite anti-persistent. This anti-persistence is due to local negative feedback associated with reactions to infection. Specifically, local protection arises as a reaction to local increases infections. The proportion protecting decreases once infections are lowered, but often does not extinguish infections, resulting in oscillations. Other times protection will succeed in extinguishing infections. A typical pattern close to the time of extinguishing infection is that individuals surrounding an infected person all protect, while individuals in regions with no infection defect.

Using the same initial conditions as above, except that before the game starts the lattice has 500 links rewired (as in Fig. 1d), the mean $\alpha=0.812$ (SD=0.032), ranging from 0.765 to 0.837, which shows persistence. Thus randomly rewiring a small proportion of links has the effect of shifting the incidence pattern from anti-persistence to persistence. With the rewiring, the average number of individuals protecting was only 11.6% (SD=9.6%) of the population, aggregated into a few small clusters in local areas that by chance suffered fewer rewiring of connections (see Fig. 1d for an example at 1000 time steps). Rewiring as many as 10% of links, creating a small-world network as described earlier, and α still shows persistence when the b/c ratio supports protection, which is

the case when the b/c ratio exceeds 2. By plotting α by the b/c and comparing this to the level of protection we see a striking correspondence (Fig. 5). We can understand levels of α (Panel B) in terms of levels of protection and infection (panel A). Recall that when the α for the incidence time trace is above 0.5 the incidence time trace shows more persistence, associate with disease spreading, and when it is below 0.5 the incidence shows anti-persistence which we interpret as negative feedback from protection responding to disease. So we should expect persistence where protection does not survive. Below a b/c of 2, protection does not survive, and so infection spreads unabated. That is when b/c is below 2, the spread of infection is persistent, reflecting positive feedback, because increased incidence breeds more incidence as disease spreads. Above a b/c of 5, protection has reached very close to 100% and so protection is by far the dominance response to disease incidence (negative feedback, protection reacts against incidence of disease). In the region between a b/c of 2 and 5, protection coexists with defection, as reported for Fig. 4. Comparing the levels of protection in Fig. 5 (run for 6000 iterations) to that in Fig. 4 (run for 500 iterations), 39 of the 40 points between b/c of 2 and 5 differ by less than 1%, showing that results remain stable over the long-term. In this intermediate region between a b/c of 2 and 5, higher levels of b/c support higher levels of protection but the defectors that remain are vulnerable to infection, which supports persistence of infection.

We see three main types of negative feedback, local protection mitigating infection after local infection rises, local defection rising in response to the high levels of health brought on by surges in local protection, and infection invading healthy defectors. These types of responses occur at a range of scales, largely because many different sizes of collectives grow. By contrast, if individuals learn asocially using either global prevalence or using all available local information, the negative feedback does not occur at all scales. This is because when individuals acting and evaluating alone do not imitate highest local payoff, and so collectives of various sizes do not form except directly surrounding an infected person or persons. Also, if individuals use all local information about payoffs, infection and efficacy, relatively few resulting errors (in terms of choosing lower payoff in the short run, or allowing disease to spread in the longer run, see supplementary material Figs. S2 and S3), but this type of individual asocial learning is difficult and costly (Hoppitt and Laland, 2013; Valone, 2007; Morris, 1992). When individuals only use local information about highest payoff, as in our model. then there is a local bias in addition to the bias of choosing the best. Spatially clustered networks "buffer" individuals, shield them from seeing alternative behaviors, e.g. infected defectors surrounded by other infected defectors earn payoffs of zero but see no behavioral alternative, consistent with Rendell et al's (2010) finding that spatial buffering allows spread of a behavior beneficial at the margins of clusters but not beneficial inside the clusters (Rendell et al., 2010). Another source of "mistakes" in the social learning we examined in this paper arises from the simple fact that individuals do not know what behavior their neighbors will choose, resulting in some individuals choosing to defect not knowing that if their other neighbors choose defect, they may all succumb to infection resulting in low payoff. If the b/c ratio is above 2, and so long as some protectors exist, individuals can choose to protect and therefore can correct erroneous choices to defect. Such errors are corrected over a varying lengths of time, resulting in negative feedback responses at different scales. The "noise" in incidence reflects these various errors and their corrections. This noise also is reflected visually in the multi-scale oscillations (Fig. 2) that correspond to the arising and collapsing of different sizes of collectives of protectors (Fig. 3) affecting and responding to changing levels of incidence. Although average incidence varies little, the "noise" in incidence fluctuations reflects variability about underlying protective behavior in response to disease. So long as the b/c supports protection, the "noise" in the time trace of incidence has a pattern reflecting behavioral response to disease and disease persistence.

4. Conclusions

A simple social learning strategy, adopting the highest payoff in a spatially clustered network is a sufficient explanation of chaotic patterns in disease incidence. The general network structure and learning strategy are very common among humans and animals. While this demonstrates a plausible and sufficient explanation, we cannot claim that this model is necessary or complete. Nor does the model claim to represent an elaborate learning strategy such as humans are capable of. This learning strategy is very common, although inherently biased. In fact the errors resulting from this learning strategy are an important part of the explanation for the chaotic patterns of incidence.

In this model, mistakes occur at all scales, e.g. at some time steps only a few individuals will choose a lower than optimal payoff, whereas at other times, a very large number of individuals will choose a lower and often a zero payoff (when clusters of infected individuals defect). One frequent source of small-scale mistakes is the very high but short-lived payoffs resulting from free-riding on many healthy neighbors. This locally higher payoff leads others to defect and ensuing infection extinguishes the local benefits of free-riding. A single free-riding defector, or a thin line of defectors, will earn high payoffs, leading neighbors to defect. The expansion of defectors leads to a drop in the payoff, a negative feedback. As a result, single defectors, or very small collectives of defectors, frequently expand only to shrink again, leading to small-scale surges and dips in infection.

Infection itself, when unhindered by protection would spread smoothly and steadily, consistent with positive feedback. In an area where there are only defectors, infection expands relatively steadily, accounting for some of the slower, larger scale increases in infection. If the resulting area of infected defectors eventually borders any protectors, then at that point then protection may expand steadily for a while. This expansion of protection is adaptive, at least in the short run, because it prevents disease from spreading and often contributes to higher payoff via health of individuals in one's local neighborhood. However, as health expands, so does the temptation to defect. Loner defectors earn the highest payoff, even when infected, due to free-riding. This stimulates neighbors to defect which results in the original defector earning a low payoff, or zero payoff if all defecting neighbors become infected. This negative feedback then often occurs at small scales. More generally, defectors do very well when they border many protectors, as is the case when many small islands of protectors exist. A common result is for single thin lines of defectors to exist between many small islands of protectors, but the high payoffs lead protectors to defect, which thickens the line of defectors such that many earn a payoff of zero. As a result, lines of defectors oscillate in thickness, islands of protectors oscillate in size, and their payoffs oscillate greatly. This is consistent with the observation that "imitate the best" or "imitating the most successful" can lead to widespread adoption of suboptimal strategies (Baldini, 2013; Rendell et al., 2010; Schlag, 1998; Schlag, 1999; Denrell, 2005). In the current model, imitating the best is biased towards defection. Within a block of defectors, the payoff of the infected defectors surrounded by other infected defectors is zero. Yet when the block of infected defectors is surrounded by protectors, the corner defectors in the defection block have a high payoff, which supports expansion of the block despite the zero payoff earning defectors inside the block. That corner defector borders 5 protectors (so

earns a payoff of 5*b*), which neighboring defectors will regard as "the best." The defectors focus on that high earning defector and ignore the defectors earning zeros inside the block, under the "imitate the best payoff" strategy. Now if the strategy were to choose the behavior with the highest average payoff (the average among one's neighbors, for each behavior), defection would be less attractive. That's because when averaging the payoff, the many zero payoffs of defectors would be counted, and so would lower the average score associated with defection. We would still expect oscillations to occur, when individuals adopt the behavior with the highest average payoffs, because defection would still tend to expand and then collapse, however it is very possible the oscillations would be smaller and chaos might not result. I chose to focus on imitate the best because it is a common strategy (mesoudi, 2008; Sarin and Dukas, 2009; Henrich and Broesch, 2011; Pasqualone and Davis, 2011; Seppanen et al., 2011; Mason, 1988; Kendal et al., 2009; Garcia-Retamero et al., 2009). Yet it would be interesting to study whether or not other social learning mechanisms might produce similar effects.

This model we examined in this paper explicitly includes "local" collective health, rather than just individual health, a model of public health behavior. Specifically, we assume that individuals benefit from having healthy neighbors. Each individual benefits from local health because healthy neighbors are more capable of contributing to the local welfare. Even just one individual protecting produces some benefit for both self and other even if no one else protects. This is not the case in the famous prisoner's dilemma game, in which one cooperator can produce no benefit alone (a greater social dilemma and more difficult to overcome), and in this respect a less common situation than the milder form of dilemma seen in this infection–protection game. The infection–protection game differs from other game models, furthermore, because the threat to welfare is a condition that spreads through finite network structures. The small-world network structure, relative to the lattice network (a large world network), has an interesting effect on the relative mix of protectors and defectors due to the infection dynamics in the model. Clusters of healthy defectors often form in the lattice network. Within these clusters defectors earn the highest payoff possible. Rewiring the lattice to form a small-world network lowers the average path length, and so helps the spread of infection through defectors, undermining the health of defectors. As a result, we see higher proportions of protection in small-world networks at all levels of infection, but particularly for very low levels of infectivity (less than 10% infectivity), because at this low level of infectivity, protection rarely survives in a straight lattice network. Thus population structure matters in this game.

The dynamics of spreading condition in this game could be modified to represent some other spreading threat, e.g., a spread of some resource deleting condition, a military invasion, spread of some attitude, or a natural condition such as floods or forest fires (the size and frequency of these disasters follows power law frequency distributions (Malamud, 2004; Malamud and Turcotte, 1996; Malamud et al., 1998)). In all these case, the short-term value of protection is conditional upon presence of a threat. This draws attention to that cooperation may be conditional not only upon what others are doing, but also upon the conditions such as the presence of a disease or other threat.

The game leads to collectives of protection that control the spread of disease and also lead to fractal time trends in protective behavior and disease incidence. The exponential frequency distribution of the sizes of protective collectives, is consistent with deterministic chaos seen in nonlinear systems (Sigeti, 1995; Ohtomo et al., 1995; Brandstater and Swinney, 1987). Nature offers many examples of these types of spatial and temporal patterns, e.g. heart rhythms (Babloyantz and Destexhe, 988.), flame front dynamics (Elhamdi et al., 1993), plasma dynamics (Maggs and Morales, 1993), and a variety of natural disasters (Malamud, 2004). Incidence of some childhood diseases shows multi-scale fractal irregularity over time (Holdsworth et al., 2012) or simpler oscillations (Holdsworth et al., 2012; May, 2000; Manfredi et al., 2009; Bauch and Earn, 2004). Several studies of "noise" in fluctuations of disease patterns, notably rotavirus (Jose and Bishop., 2003), campylobacter (Skjerve and Glattre, 2006), measles (Bolker and Grenfell, 1996) some cancers (Nygard and Glattre, 2003), revealed fractal patterns that may contain information regarding the underlying dynamics. However, it is very difficult to tease out from empirical data chaotic patterns arising from stochasticity from that arising from deterministic non-linear systems (Addison, 1997). By contrast, an individual-based agent based simulation such as I present in this paper may explain underlying feedback associated with social learning that can give rise to chaotic patterns in health protection and disease. The infection–protection game model provides a possible cause of fractal temporal patterns. It is conceivable that adding stochasticity could either add fractal oscillations patterns where it did not previously exist in the purely deterministic model, or that it could actually remove those fractal oscillations. However, the fractal patterns were evident in the both the deterministic and stochastic versions. Even the deterministic version produces fractal time traces of infection with $\alpha < 0.5$ ($D > 1.5$), indicating some anti-persistence suggesting presence of negative feedback. Note for comparison $\alpha = 0.29$ was found in campylobacter trends (Skjerve and Glattre, 2006). For rotavirus time-series (Jose and Bishop., 2003), which can fit an SIS dynamic (White et al., 1998), α takes on different values for different time scales within the trace, e.g. for scales less than a year $\alpha = 1.08$, between 1 and about 3 years $\alpha = 0.23$ (anti-persistence), and between 3 and about 5 years $\alpha = 0.64$ (persistence). The overall dynamics of rotavirus (Merler et al., 2008) show a time trend pattern similar to the output of the infection–protection model. Jose and Bishop. (2003). The infection–protection model not only approximates an SIS model but also, more uniquely, contains an explicit behavioral negative feedback mechanism (social comparison selection of protective behavior). Prior literature has not offered a model of the mechanisms giving rise to the fractal scaling observed in time series of several diseases. Some epidemiological studies offer clues, e.g. that the re-infection rate correlates with the logarithm of the local incidence (Wang et al., 2007; Uys et al., 2007). However, an explicit model generating these effects awaits. Several models of the SIS process, based on difference equations, have produced repeated bifurcations leading to chaos (Das et al., 2009; Yakubu, 2007; Li and Cui, 2013), but these equation-based models cannot incorporate clustering nor individual-based learning and behavior in networks. To obtain chaotic results these prior models of SIS and also SIR use seasonal forcing, generally by increasing the contact rate during certain times, such as the beginning of the school year (Keeling et al., 2001; Schwartz, 1985; Thornley and France, 2012). By contrast, the model I presented has no forcing (seasonal or otherwise), yet produces deterministic chaotic processes even before adding stochasticity. Within a range of moderate levels of benefit-to-cost, protection, defection and infection dynamically co-exist, showing deterministically chaotic fractal patterns of cooperation in which collective health protection is exponentially more frequent in small compared to large collectives. Because individuals adapt to changing local conditions in this model, all sizes of protective collectives arise and collapse over time, leading to temporally chaotic patterns of prevalence. Analogous to the chaotic rhythm of the heart rate as a signature of healthy heart dynamics (Babloyantz and Destexhe, 988.; Peng et al., 1993; Perkiömäki et al., 2005), the chaotic time trends in behavior and infection may be a signature of adaptive local feedback.

Author contributions

Dr. Keane designed the model, conducted the analysis and wrote the manuscript.

Conflicts of interest

The author declares no conflict of interest.

Acknowledgments

I thank Steven Albert, Robert Harper, and Chelsea Pallatino, for commenting on earlier versions of this paper.

Appendix A. Supporting information

Supplementary data associated with this article can be found in the online version at http://dx.doi.org/10.1016/j.jtbi.2016.08.039.

References

Aberg Yngwe, M., Fritzell, J., Lundberg, O., Diderichsen, F., Burstrom, B., 2003. Exploring relative deprivation: is social comparison a mechanism in the relation between income and health? Soc. Sci. Med. 57 (8), 1463–1473.
Addison, P., 1997. Fractals and Chaos: An Illustrated Course. Institute of Physics Publishing, London.
Ajzen, I., 1991. The theory of planned behavior. Organ. Behav. Hum. Decis. Process. 50, 179–211.
Ajzen, I., Fishbein, M., 1980. Understanding Attitudes and Predicting Social Behavior. Prentice-Hall, Englewood Cliffs, NJ.
Al-Tawfiq, J., Pittet, D.D., 2013. Improving hand hygiene compliance in healthcare settings using behavior change theories: reflections. Teach. Learn Med. 25 (4), 374–382.
Anonymous, 2006. Condoms and the Vatican. Lancet 367, 1550.
Arden, M., Armitage, C., 2008. Predicting and explaining transtheoretical model stage transitions in relation to condom-carrying behaviour. Br. J. Health Psychol. 13 (4), 719–735.
Babloyantz, A., Destexhe, A., 1988. Is the normal heart a periodic oscillator. Biol. Cyber. 58 (3), 203–211.
Baldini, R., 2013. Two success-biased social learning strategies. Theor. Popul Biol. 86, 43–49.
Bauch, C., Earn, D., 2004. Vaccination and the theory of games. Proc. Natl. Acad. Sci. USA 101, 13391–13394.
Berkman, L., Glass, T., 2000. Social integration, social networks, social support, and health. In: Berkman, L., Kawachi, I. (Eds.), Social Epidemiology. Oxford University Press, New York, pp. 137–173.
Berkman, L., Kawachi, I., 2000. Social Epidemiology. Oxford University Press, New York.
Bolker, B., Grenfell, B., 1996. Impact of vaccination on the spatial correlation and persistence of measles dynamics. P. Nat. Acad. Sci. USA 93, 12648–12653.
Boyd, R., Richerson, P., 1985. Culture and the Evolutionary Process. Chicago University Press, Chicago.
Brandstater, A., Swinney, H., 1987. Strange attractors in weakly turbulent Couette–Taylor flow. Phys. Rev. A 35 (5), 2207–2220.
Brauer, F., Castillo-Chavez, C., 2012. Chapter 10. Models for Endemic Diseases. In: Mathematical Models in Population Biology and Epidemiology. Texts in Applied Mathematics, Vol. 40, pp. 411–464.
Centola, D., 2010. The spread of behavior in an online social network experiment. Science 329, 1194–1197.
Christakis, N., Fowler, J., 2009. Connected: The Surprising Power of our Social Networks and How they Shape our Lives. Little Brown and Co, New York.
Coates, A., Ng, A., 2012. Learning Feature Representations with K-Means. In: Neural Networks: Tricks of the Trade. Springer, New York.
Crosby, R., Yarber, W., Sanders, S., Graham, C., 2005. Condom discomfort and associated problems with their use among university students. J. Am. Coll. Health 54, 143–147.
Das, P., Mukandavire, Z., Chiyaka, C., Sen, A., Mukherjee, D., 2009. Bifurcation and chaos in S-I-S epidemic model. Differ. Equ. Dyn. Syst. 17 (4), 393–417.
Denrell, J., 2005. Should we be impressed with high performance? J. Manag. Inq. 14 (3), 292–298.
Dubbert, P., Dolce, J., Richter, W., Miller, M., Chapman, S., 1990. Increasing ICU staff handwashing: effects of education and group feedback. Infect. Control Hosp. Epidemiol. 11, 191–193.
Elhamdi, M., Gorman, M., Robbins, K., 1993. Deterministic chaos in laminar premixed flames—experimental classification of chaotic dynamics. Combust. Sci. Technol. 94, 87–101.
Ferng, Y., Wong-McLoughlin, J., Barrett, A., Currie, L., Larson, E., 2011. Barriers to mask wearing for influenza-like illnesses among urban Hispanic households. Public Health Nurs. 28, 13–23.
Festinger, L., 1954. A theory of social comparison processes. Hum. Relat. 7 (2), 117–140.
Funk, S., Salathé, M., Jansen, V., 2010. Modelling the influence of human behavior on the spread of infectious diseases: a review. J. R. Soc. Interface 7 (50), 1247–1256.
Garcia-Retamero, R., Takezawa, M., Gigerenzer, G., 2009. Does imitation benefit cue order learning? Exp. Psychol. 56, 307–320.
Glanz, K., Rimer, B., Lewis, F., 2002. Health behavior and health education, Theory, Research and Practice, San Fransisco. Wiley & Sons.
Goldmann, D., 2001. Epidemiology and prevention of pediatric viral respiratory infections in health-care institutions. Emerg. Infect. Dis. 7 (2), 53–80.
Henrich, J., Broesch, J., 2011. On the nature of cultural transmission networks: evidence from Fijian villages for adaptive learning biases. Philos. Trans. R. Soc. B 366, 1139–1148.
Hjorth, A., Head, B., Wilensky, U., 2014. NetLogo K-Means Clustering model. Center for Connected Learning and Computer-Based Modeling, Northwestern University, Evanston, IL. ⟨http://ccl.northwestern.edu/netlogo/models/K-MeansClustering⟩.
Holdsworth, A., Nicholas, K., Kevlahan, N., Earn, D., 2012. Multifractal signatures of infectious diseases. J. R. Soc. Interface 9 (74), 2167–2180.
Hoppitt, W., Laland, K., 2013. Social Learning: An Introduction to Mechanisms, Methods, and Models. Princeton: Princeton University Press.
Jackson, M., 2008. Social and Economic Networks Vol. 3. Princeton University Press, New York: Princeton.
Jose, M., Bishop, R.F., 2003. Scaling properties and symmetrical patterns in the epidemiology of rotavirus infection. Philos. Trans. Roy. Soc. Lond. B 358, 1625–1641.
Kanungo, T., Mount, D., Netanyahu, N., Piatko, C., Silverman, R., Wu, A., 2002. An efficient k-means clustering algorithm: Analysis and implementation. IEEE Trans. Pattern Anal. Mach. Intell. 24, 881–892.
Kearns, M., 2007. Graphical games. Algorithm. Game Theory 3, 159–180.
Kearns, M., Suri, S., 2006. Networks preserving evolutionary equilibria and the power of randomization. In: Proceedings of the 7th ACM Conference on Electronic Commerce. ACM Press, Ann Arbor, pp. 200–207.
Keeling, M., Rohan, I., Grenfel, B., 2001. Seasonally forced disease dynamics explored as switching between attractors. Physica D 148, 317–335.
Kendal, J., Giraldeau, L., Laland, K., 2009. The evolution of social learning rules: payoff-biased and frequency-dependent biased transmission. J. Theor. Biol. 260, 210–219.
King, B., Scott, T., Wajeeh, S., 2005. Factors affecting individuals dissuading sexual partners from using condoms: a comment on McDermott and Noland. Psychol. Rep. 96, 586–590.
Kuzu, N., Ozer, F.F., Aydemir, S., Yalcin, A., Zencir, M., 2005. Compliance with hand hygiene and glove use in a university-affiliated hospital. Infect. Control Hosp. Epidemiol. 26 (3), 312–315.
Larson, E., 1985. Handwashing and skin: physiologic and bacteriologic aspects. Infect. Control 6, 14–23.
Lefkowitz, E., Gillen, M., Shearer, C., Boone, T., 2004. Religiosity, sexual behaviours and sexual attitudes during emerging adulthood. J. Sex. Res 41, 150–159.
Li, J., Cui, N., 2013. Bifurcation and chaotic behavior of a discrete-time SIS model. Discret. Dyn. Nat. Soc.
Lieberman, E., Hauert, C., Nowak, M., 2005. Evolutionary dynamics on graphs. Nature 433 (7023), 312–316.
MacIntyre, C., Cauchemez, S., DE, D., 2009. Face mask use and control of respiratory virus transmission in households. Emerg. Infect. Dis. 15, 233–241.
Maggs, J., Morales, G., 1993. Exponential power spectra, deterministic chaos and Lorentzian pulses in plasma edge dynamics. Plasma Phys. Control. Fusion 54, 124041.
Malamud, B., 2004. Tails of natural hazards. Phys. World 17 (8), 31–35.
Malamud, B., Turcotte, D., 1996. The applicability of power-law frequency statistics to floods. J. Hydrol. 322, 168–180.
Malamud, B., Morein, G., Turcotte, D., 1998. Forest fires: an example of self-organized critical behavior. Science 281, 1840–1842.
Manfredi, P., Posta, P., d'Onofrio, A., Salinelli, E., Centrone, F., Meo, C., Poletti, P., 2009. Optimal vaccination choice, vaccination games, and rational exemption: an appraisal. Vaccine 28 (1), 98–109.
Marsden, P., 1987. Core discussion networks of Americans. Am. Sociol. Rev. 52 (1), 122–131.
Mason, J., 1988. Direct and observational learning by redwing blackbirds. In: Galef, B., Zentall, T. (Eds.), Social Learning: Psychological and Biological Perspectives. Lawrence Erlbaum, Hillsdale, NJ.
May, R., 2000. Simple rules with complex dynamics. Science 287 (5453), 601–602.
Merler, S., Poletti, P., Ajelli, M., Caprile, B., Manfredi, P., 2008. Coinfection can trigger multiple pandemic waves. J. Theor. Biol. 254, 499–507.
mesoudi, A., 2008. An experimental simulation of the 'copy-successful-individual' cultural learning strategy. Evol. Hum. Behav. 29, 350–363.
Morris, D., 1992. Scales and costs of habitat selection in heterogeneous landscapes. Evol. Ecol. 1, 379–388.
Naar-King, S., Rongkavilit, C., Wang, B., Wright, K., Chuenyam, T., Lam, P., Phanuphak, P., 2008. Transtheoretical model and risky sexual behaviour in HIV + youth in Thailand. AIDS Care 20 (2), 198–204.
Noar, S., Morokoff, P., Redding, C.C., 2000. An examination of transtheoretical

predictors of condom use in late-adolescent heterosexual men. J. Appl. Biobehav. Res. 6 (1), 1–26.
Nowak, M., 2004. Evolutionary Dynamics. Oxford University Press, New York.
Nowak, M., May, R., 1992. Evolutionary games and spatial chaos. Nature 359, 826–829.
Nygard, J., Glattre, E., 2003. Fractal analysis of time series in epidemiology: is there information hidden in the noise? Nor. Epidemiol. 13, 303–308.
Ohtomo, N., Tokiwano, K., Tanaka, Y., Sumi, A., Terachi, S., Konno, H., 1995. Exponential characteristics of power spectral densities caused by chaotic phenomena. J. Phys. Soc. Jpn. 64 (4), 1104–1113.
Ohtsuki, H., Lieberman, E., Hauert, C., Nowak, M., 2006. A simple rule for the evolution of cooperation on graphs and social networks. Nature 433, 502–505.
Ohtsukia, H., Nowak, M., 2008. Evolutionary stability on graphs. J. Theor. Biol. 251, 698–707.
Pascual, M., Roy, M., Laneri, K., 2011. Simple models for complex systems: exploiting the relationship between local and global densities. Theor. Ecol. 4, 211–222.
Pasqualone, A., Davis, J., 2011. The use of conspecific phenotypic states as information during reproductive decisions. Anim. Behav. 82, 281–284.
Peng, C., Mietus, J., Hausdorff, J., Havlin, S., Stanley, H., Goldberger, A., 1993. Long-range anti-correlations and non-Gaussian behavior of the heartbeat. Phys. Rev. Lett. 70, 1343–1346.
Perkiömäki, J., Mäkikallio, T., Huikuri, H., 2005. Fractal and complexity measures of heart rate variability. Clin. Exp. Hypertens. 27 (2–3), 149–158.
Pittet, D., Mourouga, P., Perneger, T., 1999. Compliance with handwashing in a teaching hospital. Ann. Intern Med 130, 126–130.
Prochaska, B.S.C.R.V.B.N.P.M.L.F.-R.M. a J.P.J.J., 2008. Initial efficacy of MI, TTM tailoring, and HRI's in multiple behaviors for employee health promotion. Prev. Med. 46 (3), 226–231.
Prochaska, J., Velicer, W., 1997. The transtheoretical model of health behavior change. Am. J. Health Promot 12 (1), 38–48.
Rendell, L., Fogarty, W.C.M., Enquist, K., Eriksson, K., et al., 2010. Why copy others? Insights from the social learning strategies tournament. Science 327, 208213.
Salathé, M., Jones, J., 2010. Dynamics and control of diseases in networks with community structure. PLoS Comput. Biol. 6 (4), e1000736.
Sarin, S., Dukas, R., 2009. Social learning about egg laying substrates in fruit flies. Proc. R. Soc. B 276, 4323–4328.
Sarkar, N., 2008. Barriers to condom use. Eur. J. Contracept. Reprod. Health Care 13 (2), 114–122.
Schenker, J., Rabenou, V., 1993. Contraception: traditional and religious attitudes. Eur. J. Obstet. Gynecol. Reprod. Biol. 49, 15–18.
Schlag, K., 1998. Why imitate, and if so, how? A boundedly rational approach to multi-armed bandits. J. Econ. Theory 78, 130–156.
Schlag, K., 1999. Which one should I imitate? J. Math. Econ. 31, 493–522.
Schwartz, I., 1985. Multiple recurrent outbreaks and predictability in seasonally forced nonlinear epidemic models. J. Math. Biol. 18, 233–253.
Seppanen, J., Forsman, M., Monkkonnen, M., et al., 2011. New behavioral trail adopted or rejected by observing heterospecific tutor fitness. Proc. R. Soc. B. 278, 1736–1741.
Shin, S., Moey, T., 2014. The use of facemasks to prevent respiratory infection: a literature review in the context of the Health Belief Model. Singap. Med J. 55 (3), 160–167.
Sigeti, D., 1995. Survival of deterministic dynamics in the presence of noise and the exponential decay of power spectra at high-frequency. Phys. Rev. E 52 (3), 2443–2457.
Skjerve, E., Glattre, E., 2006. Fractal phenomena and fractal analysis in epidemiological studies. In: Proceedings of the 11th International Symposium on Veterinary Epidemiology and Economics.
Syed, Q., Sopwith, W., Regan, M., Bellis, M., 2003. Behind the mask. Journey through an epidemic: some observations of contrasting public health responses to SARS. J. Epidemiol. Community Health 57 (11), 855–856.
Telesford, Q., Joyce, K., Hayasaka, S., Burdette, J., Laurienti, P., 2011. The ubiquity of small-world networks. Brain Connect 1 (5), 367–375.
Thornley, J., France, J., 2012. Dynamics of single-city influenza with seasonal forcing: from regularity to chaos. ISRN Biomath.
Uys, P., van Helden, P., Hargrove, J., 2007. Tuberculosis re-infection rate as a proportion of total infection rate correlates with the logarithm of the incidence rate: a mathematical model. J. R. Soc. Interface 6 (30), 11–15.
Valone, T., 2007. From eavesdropping on performance to copying the behavior of others: a review of public information use. Behav. Ecol. Socio. 62 (1), 1–14.
Voss, A., Widmer, A., 1997. No time for handwashing!? Handwashing versus alcoholic rub: can we afford 100% compliance?. Infect. Control Hosp. Epidemiol. 18 (3), 205–208.
Wang, J., Lee, L., Lai, H., Hsu, H., Liaw, Y., Hsueh, P., Yang, P., 2007. Prediction of the tuberculosis re-infection proportion from the local incidence. J. Infect. Dis. 196 (2), 281–288.
Watts, D., Strogatz, S., 1998. Collective dynamics of 'small-world' networks. Nature 393, 440–442.
Weiss, M., Weiss, P., Weiss, D.D., Weiss, J., 2007. Disrupting the transmission of influenza a: face masks and ultraviolet light as control measures. Am. J. Public Health 97 (51), S32–S37.
White, L., Cox, M., G, M., 1998. Cross immunity and vaccination against multiple microparasite strains. IMA J. Math. Appl Med Biol. 15 (3), 211–233.
Wilensky, U., 1999. NetLogo. Evanston, IL: Center for Connected Learning and Computer-Based Modeling, Northwestern Institute on Complex Systems ⟨http://ccl.northwestern.edu/netlogo/⟩.
Yakubu, A., 2007. Allee effects in a discrete-time SIS epidemic model with infected newborns. J. Differ. Equ. Appl. 13 (4), 341–356.
Zhou, W., 2005. Discrete hierarchical organization of social group sizes. Proc. Biol. Sci. 272 (1561), 439–444.